

MIT Open Access Articles

Electric Arc Holes in Corrugated Stainless Steel Tubing

The MIT Faculty has made this article openly available. **Please share** how this access benefits you. Your story matters.

Citation: Taylor, Richard H. et al. "Electric Arc Holes in Corrugated Stainless Steel Tubing." *Fire Technology* 53, 5 (June 2017): 1919–1932 © 2017 Springer Science+Business Media New York

As Published: <http://dx.doi.org/10.1007/s10694-017-0663-1>

Publisher: Springer-Verlag

Persistent URL: <http://hdl.handle.net/1721.1/111072>

Version: Author's final manuscript: final author's manuscript post peer review, without publisher's formatting or copy editing

Terms of use: Creative Commons Attribution-Noncommercial-Share Alike



Electric Arc Holes in Corrugated Stainless Steel Tubing

Richard H. Taylor
77 Massachusetts Ave. 4-142
Department of Materials Science and Engineering
Cambridge, MA 02139
(617) 733-2280
rhtaylor@mit.edu

Harold R. Larson
77 Massachusetts Ave. 4-142
Department of Materials Science and Engineering
Cambridge, MA 02139
hrlarson@mit.edu

Thomas W. Eagar
77 Massachusetts Ave. 4-144
Department of Materials Science and Engineering
Cambridge, MA 02139
tweagar@mit.edu

ASBTRACT

Corrugated stainless steel tubing (CSST) has become a common product installed in new and retrofitted older homes. The ease of installation due to its flexibility and the need for fewer joints significantly lowers labor costs. Despite the advantages of lower cost and ease of installation, however, the thin wall of CSST presents an increased risk of perforation by both mechanical puncturing and electrical arcing from either household current or lightning strikes. In the course of forensic investigations of household fires, perforated tubing is occasionally identified as a potential cause. The metallurgical features of the perforated area are capable of distinguishing the cause of the hole as being from either lightning current or household current.

Over the last two decades, the use of corrugated stainless steel tubing (CSST) has gained popularity in residential and commercial gas systems. Originally sold in Japan as a seismically stable alternative to black iron pipe, domestic use of CSST has grown because of the ease and speed of installation. CSST requires far fewer joints than black iron pipe (which represents a theoretical reduction in leak paths) and circumvents the laborious process of threading and fitting rigid pipe joints. Manufacturers report sales in excess of 800 million feet in over 6 million homes since introduction to the U.S. market in 1990 (CSST Safety, 2011).

Unfortunately, improvement in one area often leads to a deficiency in another. The ease of installation and seismic stability of CSST comes at a cost. Typical wall thicknesses of CSST are on the order of 0.25 mm while black iron pipe is about ten times as thick, or approximately 2.5 mm. A consequence of this difference is an increased susceptibility to perforation by electrical failures and lightning strikes, especially the first-generation

yellow-jacketed CSST. The higher thermal mass of black pipe relative to CSST leaves it essentially impervious to failure in the event of a home electrical failure or lightning strike; CSST, on the other hand, can be punctured relatively easily by electrical discharge from residential circuits. However, initiating the arc without modification of the piping is not possible with low voltage supplies due to the insulating plastic jacket that can withstand potentials of tens of kilovolts¹. Arcing due to lightning (a high-voltage event) on the other hand requires no modification of the piping.

The lightning event can melt or even ablate the stainless steel tubing causing highly energized spatter, which in turn can lead to gas leaks, ignition, and gas-fueled fires. The presence of the yellow plastic jacket *during* the perforation event may capture a "halo" of molten metal around the perimeter of the hole (Figure 1). We have at times observed CSST collected from house fires with the insulating jacket still covering the perforation. Given the known voltage of the household electrical system and the correlation of lightning activity around the time of the incident, the only plausible origin of such a high-voltage energy source is lightning.

Work done in the 1940s showed that the resistance of metal to perforation by lightning decreases dramatically as the metal thickness is reduced (Hagenguth, 1949). Stainless steel of a thickness of 0.25 mm (equal to the thickness of CSST) is easily punctured, requiring an electrical discharge of less than 0.2 Coulombs, based on Hagenguth's work. The majority of lightning flashes exceed 5 Coulombs; hence a discharge of a magnitude capable of perforating CSST is probable from both positive and negative lightning flashes.

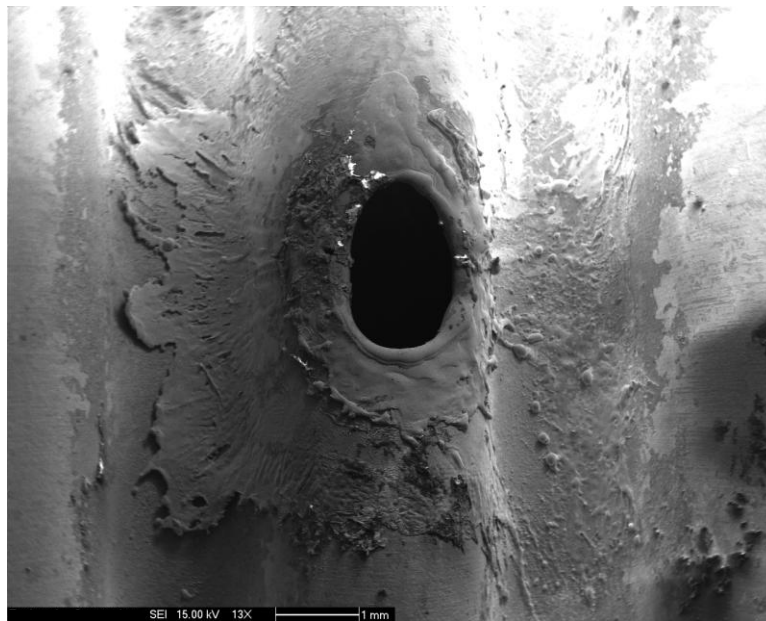


Figure 1 Lightning induced perforation of CSST showing the formation of a 'halo' of metal formed by the presence of the insulating jacket during the arc event.

¹ In lab tests (120 VAC, 20 Amp breaker) the low voltage supply arcs were produced by feeding a copper guide wire past the insulating jacket to the CSST.

Black iron pipe, which is more than 10 times the thickness of CSST would require a discharge approximately 500-1000 times larger than that required to perforate a similar size hole in CSST. The resistance of thicker metal to perforation by lightning increases due to the increased mass and fluctuation of the arc root from self-magnetohydrodynamic forces. Experimental data obtained from direct strikes on metal surfaces shows that strikes of 40 Coulombs and 90 Coulombs were unable to perforate metal thicknesses of 1.27 mm (stainless steel) and 2.03 mm (copper) respectively [M. A. Uman, Lighting Protection at the Yucca Mountain Waste Storage Facility, 2008]. The results of these triggered lightning experiments show that at over 2.5 mm thickness, black iron pipe will withstand perforation by the vast majority of direct strikes. Statistics of the parameters of lightning discharges provide that the majority of direct strikes deposit much less than 40 Coulombs [Berger, K., Anderson, R.B., and Kroninger, H. 1975. Parameters of Lightning Flashes. Electra 80: 223-237].

Of the approximately 60 million homes that currently have gas service, roughly 10 percent have a CSST-based delivery system. This statistic represents a significant quantity of at-risk homes and residents. CSST manufacturers estimate 100 lightning induced fires per year. The number of claims against CSST manufactures has grown with product exposure and reported CSST failures have led to substantial monetary losses and death. Litigation revolving around the CSST issue has spurred manufacturers to introduce design alternatives and has prompted an ongoing discussion related to the efficacy of CSST bonding as a preventative measure against electrical damage (Haslam, Galler, & Eagar, 2016).

The purpose of this paper is to introduce several metallurgical features that distinguish a puncture caused by high-frequency lightning from that caused by an electrical short in a typical residential circuit, or low-voltage 60 Hz arc (Figure 2). In the course of a forensic analysis, the ability to distinguish between these two failure modes can be critical to reconstructing the failure scenario and to the determination of the root cause of the failure.

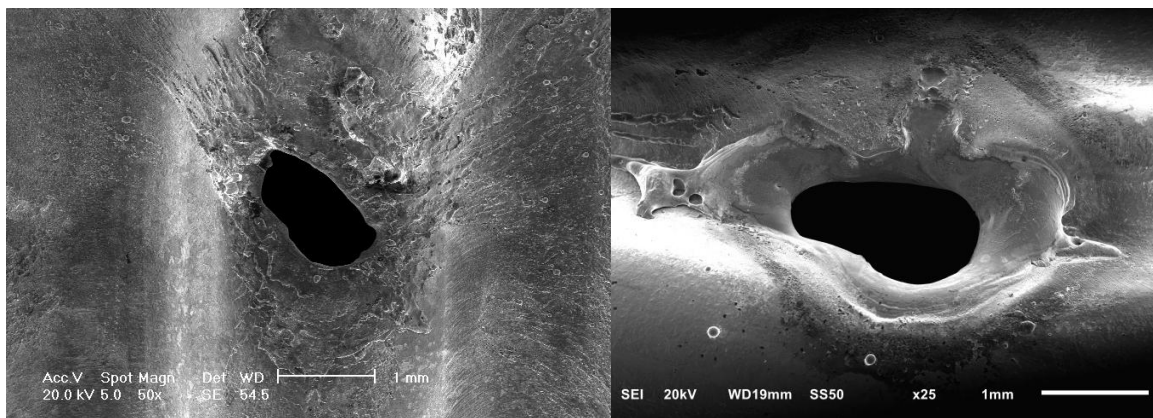


Figure 2 Left: CSST collected from lightning-related fire damage in Florida, USA. Right: CSST hole produced by a low-voltage (120VAC) supply.

The underlying physics of arcs and solidification of metal lead to distinct features that distinguish high-frequency lightning holes from those caused by much lower frequency, low-voltage arcing. The characteristic features can be identified using microscopy and can be explained in terms of the orders-of-magnitude differences between a lightning arc event

(microseconds) and a low-voltage arc event such as a short-circuited residential circuit breaker (milliseconds).

Arc Strikes

The waveform of a residential circuit arc event is largely influenced by the alternating voltage frequency of the supply. To sustain an arc, a minimum voltage determined by the distance between electrodes and the dielectric medium is required. Across any appreciable distance in air the duration of the arc is limited to about half the period of the waveform, as it is susceptible to an outage near a change in polarity. Thus, the duration of an arc event over a residential circuit is on the order of 5-10 milliseconds, with a standard U.S. supply frequency of 60 Hertz. Additionally, initiation of the arc requires an initial low resistance path (e.g., an exploding guide wire, or transient contact between the electrodes).

A cloud-to-ground lightning strike is defined by three features: 1) dart-leader and return-stroke sequences 2) continuing current and 3) M-components. Different durations and current amplitudes characterize each of these features. Negative discharge from cloud to ground (so-called "downward negative") is believed to account for approximately 90% of global cloud-to-ground lightning (Rakov & Uman, 2003). The remaining approximately 10% of strikes are "downward positive" in which positive charge is transferred from cloud to ground. Compared to negative lightning, positive lightning is characterized by significantly higher average voltages and peak currents as a consequence of the greater separation between the ground and the dense positive charge regions of cloud formations.

The primary feature responsible for lightning damage is the dart-leader-return-stroke sequence. These exhibit i) the largest peak currents, ii) the maximum rate of change of current, and iii) the greatest capacity for Joule heating as quantified by the action integral, A ,

$$A \equiv \int I^2 dt$$

The action integral, which has units of Amperes squared multiplied by Ohm seconds, is derived from the time integral of the power dispersed in an Ohmic material with resistance of 1 Ohm. Thus, it is proportional to the total heat energy deposited in the medium and can be expressed in equivalent units of Joules. In a short time event, the thermal diffusivity of even good conductors is too low to prevent localized Joule heating. The time-scale of diffusion can be estimated using the Fourier heat equation with a constant-temperature surface boundary.

$$t \sim \frac{x^2}{4\alpha}$$

In the case of stainless steels, which have thermal diffusivities around 0.03 cm² per second, the diffusion time-scale is 100 milliseconds for a 1 mm length. The duration of 95% of negative first return strokes is exceeded by this value by a factor of five hundred (Berger, Anderson, & Kroninger, 1975). The low-voltage circuit arc is exceeded by a factor of twenty. Such vast differences in scale persist across every characteristic feature of a lightning flash compared to a low-voltage arc event (Table 1). The expression "fast as lightning" has meaning when comparing lightning events with household power supply events.

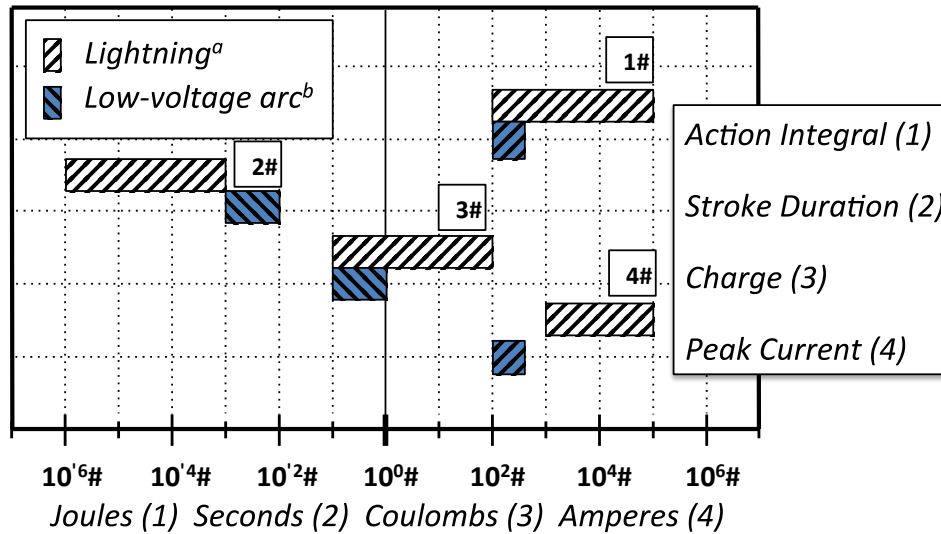


Figure 3 Differences in scale of key arc parameters in lightning and low-voltage arc. a) Lightning data taken from Berger et al. 1975. b) Range of values obtained by collecting data from 10 arcing experiments using a digital oscilloscope. Arcing events occurred on an 110V 60 Hz circuit, a 20-amp circuit breaker, and fixed iron electrodes with 25-gauge copper guide wire.

The metallurgical and physical features that reflect the large-scale differences in arc characteristics include the microstructure of the solidified region around the perimeter of the hole, the morphology of the hole perimeter and solidified melt, the extent of melt spatter beyond the perimeter of the hole and inside the tube wall, and rippling, cracking, and flow characteristics in the solidified melt.

Dendrite Arm Spacing

The microstructural features of solidified melt are known to vary with solidification conditions. In particular, *dendrite arm spacing* (DAS) varies with solidification cooling rate as

$$d = b(GR)^{-n}$$

where the cooling rate exponent n is typically near $\frac{1}{2}$ for primary dendrite arm spacing and from $\frac{1}{3}$ to $\frac{1}{2}$ for secondary dendrite arm spacing (Flemings, 1974). The pre-factor b is a material dependent factor. An exception to the form above occurs at very high cooling rates (with small primary arm spacing) for which secondary and higher-order branches may be nonexistent.

Dendrite arm spacing and its reduction with increasing cooling rate has been studied in stainless steels. Katayama et al. (Katayama & Matsunawa, 1984) determined the parameters b and n for type 310 stainless steel. Elmer (1988) extended these results in a study of seven alloys having 59 % Fe with Cr/Ni ratios ranging from 1.2 to 2.2. Thus, the results of this study reflect the behavior of a class of stainless steel alloys, including 304 stainless steel, which is commonly used for CSST.

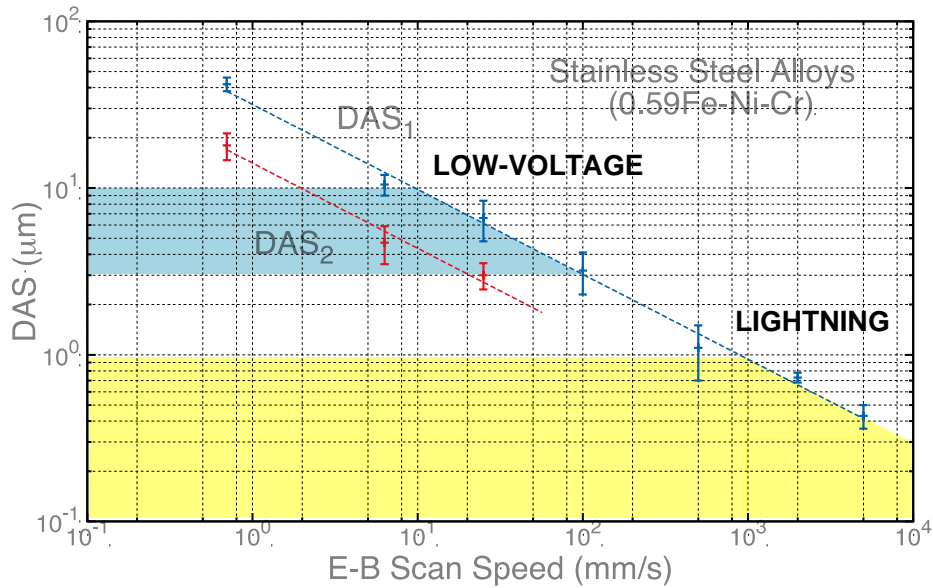


Figure 4 Primary and secondary DAS exhibit log linear dependence on electron beam scan speed. Typical low-voltage arc strike duration exceeds lightning strike duration by orders of magnitude, with accompanying difference in dendrite morphology. (After Elmer 1988)

Both lightning strike holes and low-voltage arc holes in CSST are commonly observed to have diameters in the range of 0.1-2 mm, although some lightning holes can be much larger due to the larger number of Coulombs available with lightning. Lightning and low-voltage arc event durations isolate distinct regions of the data shown in Figure 2. For lightning strikes, equivalent E-B scan speeds are from 10³ (mm/s) to 10⁶ (mm/s); thus, primary DAS will be on the order of a micron or less, and secondary dendrite arms may not form. Low voltage arc strikes, on the other hand, are as long as 10 milliseconds with equivalent E-B scan speed of 10¹-10². The primary DAS for these conditions are an order of magnitude greater, around 10 microns. During these slower events, secondary dendrite arm spacing will be more pronounced.

Thermodynamics of Hole Formation

The thermal time constants for both low-voltage events and lightning strikes permit the description of heating and melting of the hole region as an adiabatic process. The relevant physical parameters of CSST are reported below.

Table 1 Physical parameters for CSST. The value used for specific heat is an average of experimental data over a temperature range of approximately 30 °C - 1200 °C (Bogaard, Desai, Li, & Ho, 1993).

Density (kg/m ³)	Specific Heat (kJ/kg•K)	Heat of Fusion (kJ/kg)	Melting Temperature (°C)
8.03×10 ³	0.58	270	1450

The thermal energy at the hole necessary to heat and melt is the sum of several terms.

$$Q = (A_h)(d)(\rho)(C\Delta T + x\Delta H_{fus} + (1 - x)\Delta H_{ev}) + \int \sigma A_h T^4 dt$$

The radiative heat loss ($\int \sigma A_h T^4 dt$) and the latent heat of vaporization $(1 - x)\Delta H_{ev}$ (Haidar, 1998) (Zacharia, David, & Vitek, 1992) do not contribute significantly to the heat balance of the CSST hole region at these time and length scales: Radiative effects account for less than 1 millijoule per millisecond; The energy of vaporization is a more significant contributor but is still less than ½ Joule with a mass loss of less than 1% (Block-Bolten & Eagar, 1984), although for very high heat intensities, the mass loss (e.g., by ablation) can be ten times this value.

A lower bound on the energy required to melt a hole with radius of 1 mm and 0.254 mm thickness is the sum of the thermal energy to raise the temperature to melting and the thermal energy to complete the phase transition from solid to liquid. Thus, energies greater than 7 joules are required for a 1 mm radius hole in CSST.

$$\begin{aligned} Q(r = 1 [mm]) &= \left(270 \times 10^3 \left[\frac{J}{kg}\right]\right) (6.4 \times 10^{-6} [kg]) \\ &+ \left(580 \left[\frac{J}{kgK}\right]\right) (6.4 \times 10^{-6} [kg]) (1450 [K]) \\ &\cong 7 [J] \end{aligned}$$

For purposes of evaluating forensic evidence, a useful measure is the order of energy necessary to melt a CSST hole, expressed per mm² (assuming the standard thickness of ~0.254 mm): ~2.3 J/mm². This measure of energy is consistent with the experimental correlations measured by McEachron and Hagenguth in the 1940s. In that work, an approximate relation between hole size in metal sheets and lightning discharge (Coulombs) is given, wherein approximately 3 Joules produces a 1 mm² hole in metal sheet with a thickness of 10 mils (assuming a cathodic voltage drop of 10 V) (McEachron & Hagenguth, 1942).

The power deposited in the CSST by an arc event depends on the current waveform, the material work function (Φ_M), and the anodic (cathodic) voltage drop ($U_{a(c)}$). Both the anodic voltage drop and the work function are known to be near 5 V. The cathodic voltage drop is around 10 V. The power (Watts) in the CSST as a function of time (s) is then,

$$P = I(t)(U_{a(c)} + \Phi_M).$$

In the case of the low-voltage arc events, the time dependent current can be approximated as a sinusoidal waveform at 60 Hz with amplitude in the known range of values (Figure 5).

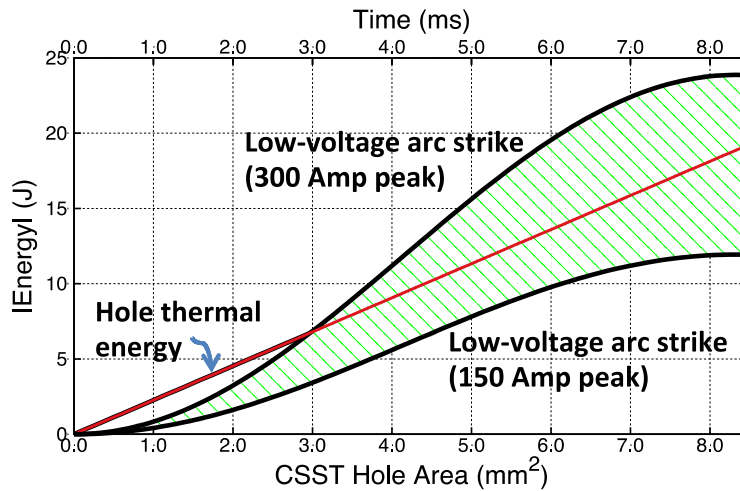


Figure 5 Approximate thermal energy for melting CSST as a function of hole area and range of low-voltage arc energy.

Cumulative energies in the vicinity of 10 Joules are generated in the time frame of the low-voltage arc event, very near the thermodynamic energy required to heat and melt a CSST hole with a diameter between 1-2mm.

In a similar vein, the return stroke waveform of a lightning flash may be modeled by a double exponential function with time constants reflecting the rapid rise time and relatively slow decay rate.

$$I(t) = I_0(e^{-at} - e^{-bt})$$

A typical wave form with peak current around 30 kA and 10 μ s rise / 30 μ s fall time constants reaches ~95% of the total power generated (~14.5 Joules) after 100 microseconds. Measured values of the first return stroke duration (2 kA to half peak of fall) range from as little as 25 μ s to 2000 μ s (Berger, Anderson, & Kroninger, 1975). In the most extreme of cases (positive flashes), the measured peak current is as high as 250 kA. Thus, stroke duration is not a limiting consideration in the formation of holes due to lightning, unlike the case of low-voltage arcs.

As shown above, the energy of a low-voltage arc can be sufficient to heat and melt a hole in the CSST *if one assumes that the arc can be initiated*. The path from an energized source in direct contact with plastic jacketed CSST will resist arc formation up to several tens of kilovolts (kV), due to the insulating properties of the polymer (Lide, 2007-2008). In the presence of a pinhole or other small defect in the dielectric sheathing, even direct proximity to an energized source – a somewhat pathological scenario – requires a voltage greater than or equal to the breakdown potential of air (~3.4 kV/mm).

With a plastic jacket thickness of approximately 1 mm or greater, low-voltage arc formation requires removal or charring of a portion of the dielectric sheathing and subsequent contact with an energized source (e.g., an exposed hot wire). Even if the conditions for a low-voltage arc are met, the presence of an arc does not preclude significant differences in the metallurgical features compared to lightning-strike holes. A characteristic feature of lightning strike holes is a region of severe splatter about the perimeter of the hole,

extending several convolutions beyond the hole location. This feature is inconsistent with the effects of a low-voltage strike due to the lower peak currents and much lower forces involved. Another feature of lightning strike holes is that they may form underneath the insulating sheath. The melting and ejection of steel under the plastic sheath often produces a characteristic "halo" of depressed, solidified metal around the perimeter of the hole (See Figure 1).

Arc Force and Hole Morphology

The force of the arc column on the molten region of the CSST varies as the square of the current. An approximate relation using the magnetohydrodynamic theory of an ideal conducting liquid shows a material-independent proportionality (Halmoy, 1979),

$$F_{arc} = \frac{\mu_0 I^2}{8\pi}$$

where μ_0 is the permeability of free space. Converti (Converti, 1981) extended this result to account for the arc expansion,

$$F_{arc} = \frac{\mu_0 I^2}{8\pi} \left(1 + 2 \ln \left(\frac{R_2}{R_1} \right) \right)$$

where R_2 is the radius of the arc at the baseplate (CSST) and R_1 is the radius of the arc at the electrode. Measurements of the force of welding arcs on the weld pool for currents between 100-350 amperes place the ratio R_2/R_1 at about 3 with measured forces between 2.5 mN – 9 mN. (Burleigh & Eagar, 1983) (Rokhlin & Guu, 1993).

It is important to note the vastly different peak forces of lightning strikes compared to low-voltage strikes. With peak currents in the tens of thousands of amperes for lightning and at most a few hundred amperes for low-voltage arcs, the associated forces (and pressures) will vary by a factor of ten thousand or more (Figure 6).

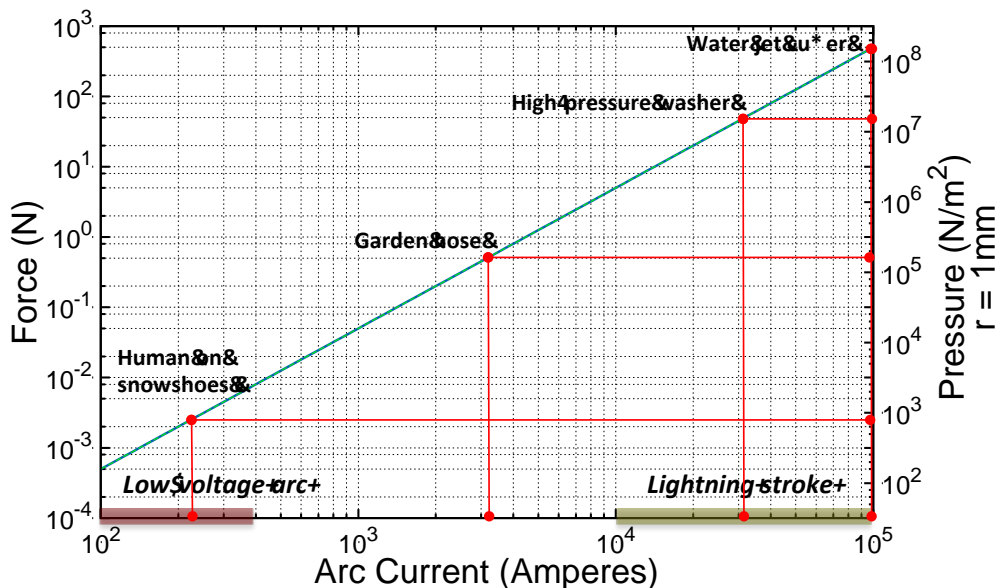


Figure 6 Arc force and pressure scale as function of current.

The measured depressions of molten metal pools produced by arcs with currents between approximately 100 - 350 amps (Rokhlin & Guu, 1993) show that: a) mass is conserved with respect to the “hump” volume and depression volume (i.e., little to no spatter is occurring from the weld pool) and b) marked pool depression is not observed until currents of ~250 amps are reached (Lin & Eagar, 1985)². Thus, the observed morphology of low current/voltage hole formation is consistent with expected morphology based on experimental and theoretical results. The melt region is not widely dispersed or scattered but reveals continuous, possibly overlapping flow patterns from the melt pool.

High Energy and Temperature Effects

Lightning strokes are capable of generating peak currents as high as 250 kA in a matter of microseconds with thermal energy greater than 100 Joules. The resultant energy density is thus sufficient to bring the steel beyond its boiling point (~2800 °C) leading to violent reactions in which thermal stresses are exceedingly high and energized steel vapor is produced. The edges of lightning induced holes may have sharp features and irregular boundaries; cracking along grain boundaries may be seen; thermal etching may be present; and melt around the hole perimeter may be minimal (Figure 7-10).

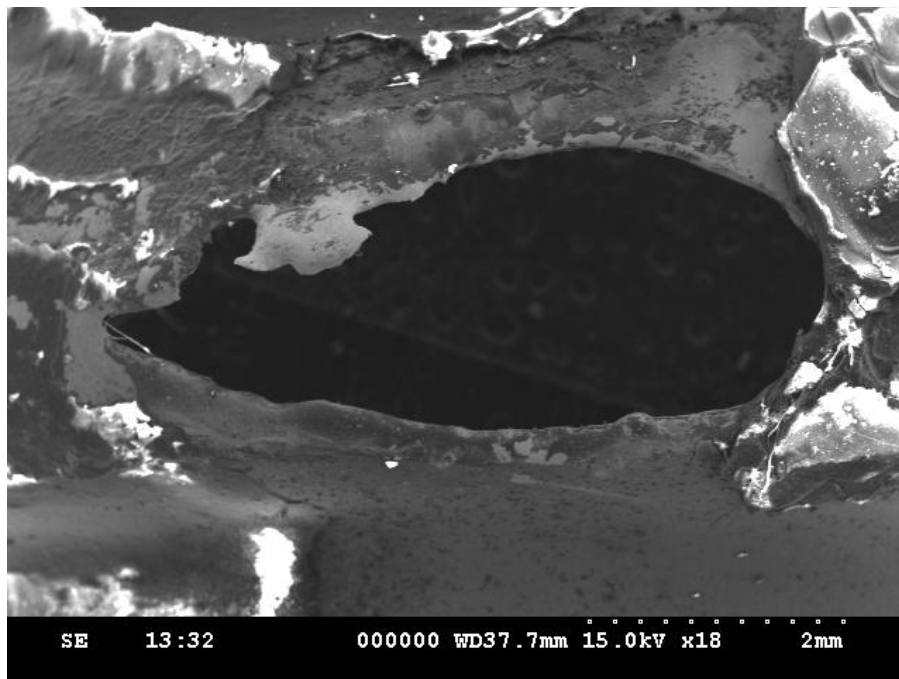


Figure 7 CSST collected from lightning-related fire damage in North Carolina, USA. The short time scale event resulted in sharp edged features around the hole perimeter.

² Note that in arc welding, virtually all spatter emanates from the consumable electrode and not from the weld pool. For example, gas tungsten arc welding produces virtually no spatter. Gas metal arc welding of steel produces significant spatter in oxidizing atmospheres due to exploding bubbles of carbon monoxide gas.

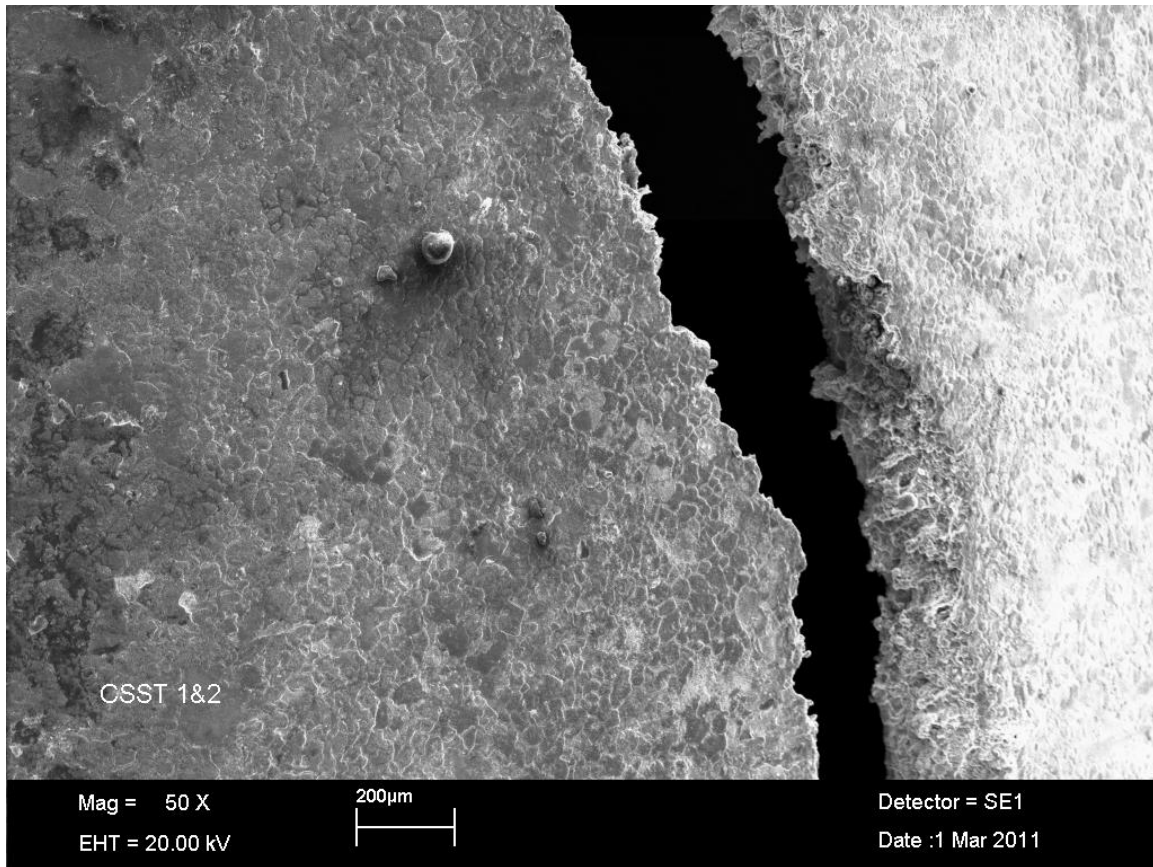


Figure 8 CSST collected from lightning-related fire damage in South Carolina, USA. Intergranular cracking and thermal etching are visible.

The thermal stress (shock) on the hole region is due to the high temperature difference induced locally in a time period on the order of microseconds. The stress σ can be computed using,

$$\sigma = Ea\Delta T$$

where E is Young's modulus (~ 180 GPa), and a is the coefficient of thermal expansion ($\sim 18 \times 10^{-6}$ m/m°C). A 100 μ s thermal time constant (pulse duration) corresponds to a thermal diffusion length of less than 50 microns. The thermal gradients under these conditions correspond to stresses on the order of 1 GPa, which exceeds the tensile strength of stainless steel.

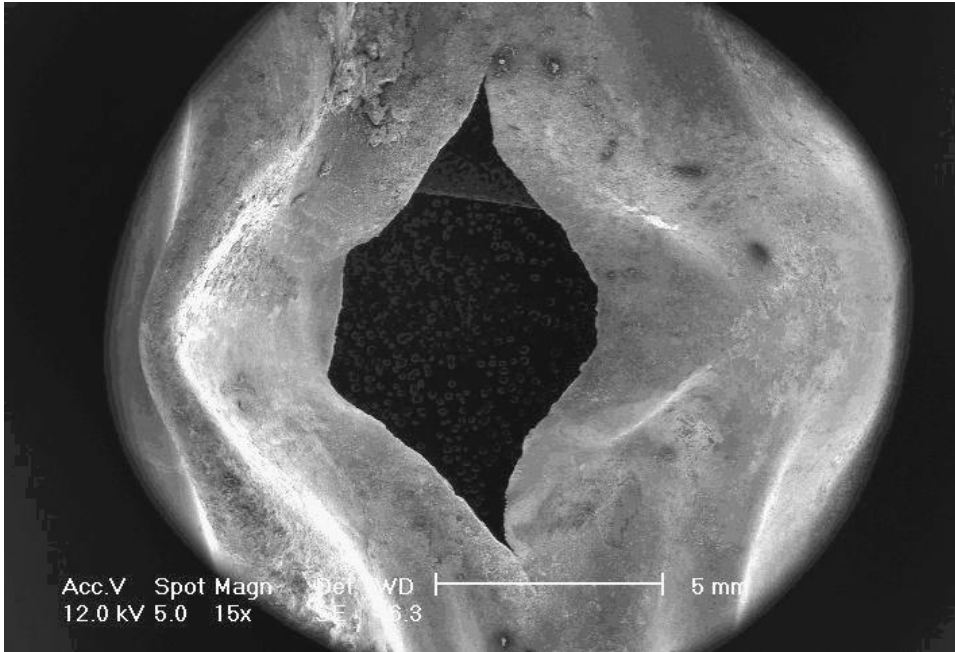


Figure 9 CSST collected from lightning-related fire damage in Florida, USA. The thermo-mechanical forces from the lightning strike resulted in a tearing of the CSST. The origin of the fracture is accompanied by molten metal spatter (Figure 9).

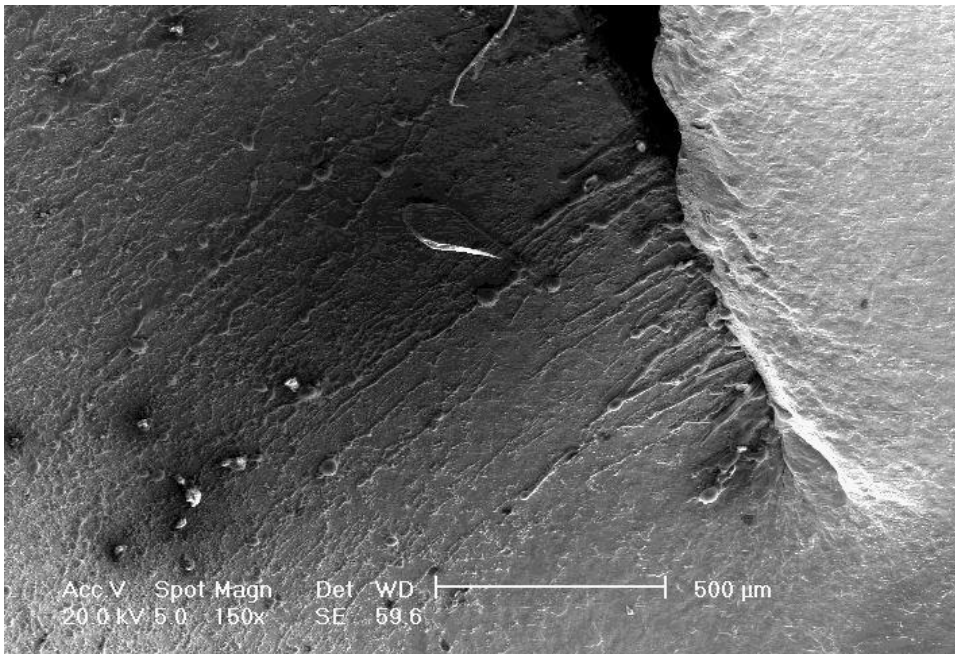


Figure 10 Fracture origin of CSST hole shown in Figure 8. Note the trails of solidified molten metal.

Conclusion

The order-of-magnitude differences in the phenomenological characteristics of lightning strikes as compared to low-voltage arcs results in unique morphological and metallurgical features in the CSST holes they produce. These features include but are not limited to:

- i) Dendrite arm spacing and pulse duration
- ii) Thermodynamic energy of hole formation and arc voltage
- iii) Non-linear arc force dependence on current and molten metal spatter
- iv) Ablation of metal and arc pressure
- v) Excess energy and vaporization of metal
- vi) Thermal shock cracking/etching

Conventional metallurgical techniques can be used to identify the characteristic features. The existence of features that distinguish high-voltage events from low-voltage events is expected because of relations that have their origins in fundamental physics and materials science. While the list above is not exhaustive, it suffices in many cases to distinguish between two failure modes, namely, the failure due to a low-voltage household electrical failure and the failure due to a high-voltage arc from a lightning strike.

It is important to note that the statistical variability in lightning discharge currents as well as the variability in duration of direct or indirect strikes means that it is not possible in every instance to distinguish between lightning damage and damage from household power by the features presented here alone. Nevertheless, *if such features are present* they are positive identification of lightning rather than household current because the phenomenological extremes of lightning are not accessible by household power. In other words, not every lightning hole will exhibit the characteristic damage, but every low-voltage hole will not. In the case of CSST damage without the characteristic features of a lightning strike, additional non-metallurgical considerations are considered, such as proximity of the hole to electrical wiring and the presence of trace metals around the hole diameter.

The ability to distinguish between these two modes is invaluable from the standpoint of a forensic/failure analysis, where a difference in root cause may lead to dramatically different event scenarios. Correctly assessing the extent of damage associated with the use of thin-walled gas tubing as well as the response of the tubing during predictable exposure scenarios is critical if usage risks are to be understood and mitigated.

Works Cited

- Berger, K., Anderson, R. B., & Kroninger, H. (1975). Parameters of Lightning Flashes. *Electra*, 80, 223-237.
- Block-Bolten, A., & Eagar, T. W. (1984). Metal vaporization from weld pools. *Metallurgical Transactions B*, 15 (3), 461-469.
- Bogaard, R. H., Desai, P. D., Li, H. H., & Ho, C. Y. (1993). Thermophysical Properties of Stainless Steels. *Thermochimica Acta*, 218, 373-393.
- Burleigh, T. D., & Eagar, T. W. (1983). Measurement of the Force Exerted by Welding Arc. *Metallurgical Transactions A*, 14A, 1223-1224.

Converti, J. (1981). Plasma-jets in arc welding. *Ph.D. dissertation* . Cambridge, Massachusetts: Massachusetts Institute of Technology.

CSST Safety. (2011). *CSST History*. Retrieved August 5, 2014, from CSST Safety: <http://www.csstsafety.com/CSST-history.html>

Flemings, M. C. (1974). *Solidification Processing*. New York: McGraw-Hill.

Hagenguth, J. M. (1949). Lightning Stroke Damage to Aircraft . *AIEE Transactions* , 68.

Haidar, J. (1998). A theoretical model for gas metal arc welding and gas tungsten arc welding. *Journal of Applied Physics* , 84 (7), 3518-3529.

Halmoy, E. (1979). The pressure of the arc acting on the weld pool. *Arc Physics and Weld Pool Behavior* .

Haslam, B., Galler, D., & Eagar, T. (2016). Fire Safety of Grounded Corrugating Stainless Steel Tubing in a Structure Energized by Lightning. *Fire Technology* , 1-26.

Katayama, S., & Matsunawa, A. (1984). Solidification Microstructure of Laser Welded Stainless Steels. *Proc. ICALEO* , 60.

Lide, D. R. (2007-2008). *Handbook of Chemistry and Physics* (88 ed.). New York: Taylor & Francis Group.

Lin, M., & Eagar, T. (1985). Influence of arc pressure on weld pool geometry. *Welding Journal* .

McEachron, K. B., & Hagenguth, J. H. (1942). Effect of Lightning on Thin Metal Surfaces. *AIEE Transactions* , 61, 559.

Rakov, V. A., & Uman, M. A. (2003). *Lightning Physics and Effects*. New York: Cambridge University Press.

Rokhlin, S. I., & Guu, A. C. (1993). A Study of Arc Force, Pool Depression, and Weld Penetration During Gas Tungsten Arc Welding. *Welding Research Supplement* , 381-390.

Zacharia, T., David, S. A., & Vitek, J. M. (1992). Effect of evaporation and temperature-dependent material properties on weld pool development. *Metall. Trans.* , 22B, 233-241.